

CAN PLANETS SURVIVE STELLAR EVOLUTION?

Eva Villaver¹ and Mario Livio

*Space Telescope Science Institute, 3700 San Martin Drive, Baltimore, MD 21218, USA;
villaver@stsci.edu, mlivio@stsci.edu*

ABSTRACT

We study the survival of gas planets around stars with masses in the range 1–5 M_{\odot} , as these stars evolve off the Main Sequence. We show that planets with masses smaller than one Jupiter mass do not survive the Planetary Nebula phase if located initially at orbital distances smaller than (3–5) AU. Planets more massive than two Jupiter masses around low mass (1 M_{\odot} on the Main Sequence) stars survive the Planetary Nebula stage down to orbital distances of ~ 3 AU. As the star evolves through the Planetary Nebula phase, an evaporation outflow will be established at the planet’s surface. Evaporating planets may be detected using spectroscopic observations. Planets around white dwarfs with masses $M_{WD} \gtrsim 0.7 M_{\odot}$ are generally expected to be found at orbital radii $r \gtrsim 15$ AU. If planets are found at smaller orbital radii around massive white dwarfs, they had to form as the result of the merger of two white dwarfs.

Subject headings: Stars:AGB and post-AGBs—Planetary Systems—white dwarfs

1. INTRODUCTION

In recent years, the quest for Jupiter-like giant planets has been extended to a completely different kind of hosts—white dwarfs (e.g. Debes & Sigurdsson 2002; Farihi et al. 2005; Friedrich et al. 2005). The underlying assumption has been that planets can survive the parent star’s evolution. Once this is accepted, the fact that white dwarfs are 10^3 to 10^4 times fainter than their main sequence progenitors opens up the possibility to observe planets through direct imaging in the infrared (Burleigh et al. 2002) where the planet emission peaks (Burrows et al. 1997; Ignace 2001).

In general, it has been assumed that planets survive to the white dwarf stage if they manage to stay in a large enough orbit to avoid engulfment by the star when the latter

¹Affiliated with the Hubble Space Telescope Division of the European Space Agency

increases its radius as it ascends the Red Giant Branch (RGB) and Asymptotic Giant Branch (AGB). Therefore, studies of the planet’s fate as the star evolves off the main sequence have generally been restricted to determining the planet’s orbit (e.g. Livio & Soker 1984; Soker 1994; Sackmann et al. 1993; Rasio et al. 1996; Rybicki & Denis 2001; Burleigh et al. 2002) or the orbit’s stability (e.g. Duncan & Lissauer 1998). However, before the star reaches the white dwarf stage, and immediately after the AGB evolution, the star evolves into the planetary nebula (PN) phase, where the stellar temperature can reach 300 000 K with luminosities of $10^3 L_{\odot}$, while emitting powerful winds.

In this paper we explore the effects of an evolving AGB and post-AGB star on an orbiting planet. In §2 we examine the planet survival during the AGB phase and the orbital changes due to the AGB mass-loss. In §3 we estimate the thermal conditions at the planet’s surface as the star increases its temperature during the PN phase. In §4 we estimate the range of parameters under which an outflow from the planet will ensue, and we estimate the planet’s evaporation rate due to thermal heating. In §5 we qualitatively discuss the planet’s reaction to mass-loss and other processes that might influence the planet’s evolution, and in §6 we discuss the planet’s overall survival. Our conclusions follow.

2. PLANET SURVIVAL DURING THE AGB PHASE

Single white dwarf progenitors are expected to have main sequence masses in the range from 1 to about $8 M_{\odot}$ mass (the upper mass limit is not well established). As these stars leave the main sequence they evolve into the RGB, Horizontal Branch, AGB, and PN phases in the Hertzsprung-Russell (HR) diagram, before descending the white dwarf cooling track. The major structural changes in the post-main sequence evolution of low- and intermediate-mass stars occur during the RGB and AGB phases. During the RGB and AGB the stellar effective temperature is always lower than its main sequence value and therefore it has no influence on the planet’s survival. However, it is during the late AGB evolution, the so-called thermal-pulsing AGB phase, that a planet’s orbit will be most influenced, since during this phase the star loses most of its initial mass and reaches its maximum radius.

The planet will spiral-in and evaporate totally (or in rare cases will accrete mass and become a close, low-mass companion to the star) if the planet’s orbital distance is within the reach of the star’s radius during the AGB phase (Livio & Soker 1984). An estimate of the maximum planet mass that can be evaporated inside an AGB envelope can be obtained by equating the location of the evaporation region (where the local sound speed in the stellar envelope matches the escape velocity from the planet’s surface) to the energy required to expel the envelope (Soker 1996, 1998; Nelemans & Tauris 1998). The value of this maxi-

imum mass is very uncertain because it depends on several factors, such as the efficiency of envelope ejection (Portegies Zwart & Yungelson 1998), which are largely unknown. Using the simplified formalism of Nelemans & Tauris (1998) we find that planets with masses less than $0.014 M_{\odot}$ or $15 M_J$ (where M_J is the Jupiter mass) will evaporate inside the envelope of an AGB star with main sequence mass of $1 M_{\odot}$. This mass limit is much higher, $\sim 120 M_J (0.11 M_{\odot})$ well into the stellar regime, if the planet (or brown dwarf) is engulfed inside the AGB envelope of a $5 M_{\odot}$ star.

We can therefore safely assume that planets less massive than $15 M_J$ that are engulfed, will be dissipated, because this limit corresponds to the temperature (and therefore planet’s escape velocity) reached inside the AGB envelope for the lowest mass stars (in the range examined here). Note that this planet mass limit is well below the mass of the brown dwarf ($52 M_J$) recently discovered by Maxted et al. (2006) orbiting an under-massive white dwarf. On the other hand, the case of total planet evaporation (for a planet in a close orbit around a solar-like star) has been proposed to explain the formation of single under-massive white dwarfs (Nelemans & Tauris 1998).

The structural changes that an AGB star undergoes in response to the dissipation of a planet in its interior are complex and have been extensively explored by Siess & Livio (1999a,b) and by Struck et al. (2002, 2004). The details of the destruction of such a planet within the stellar envelope of an AGB star are beyond the scope of the present work.

2.1. The Evolution of the Planet’s Orbit

In the following we concentrate on Jupiter-like planets in orbits that *avoid* engulfment when the radius of the AGB star expands during the thermal pulses, and we explore the conditions under which the planet will remain outside the stellar surface.

For orbital distances larger than the stellar radius, R_* , there is still a range of orbits for which drag effects (gravitational and tidal) are important in decreasing the planet’s orbit, ultimately causing the planet to spiral into the AGB envelope. While the gravitational drag, caused by the increase in the planet mass through the accretion of material from the stellar wind, is negligible for Jupiter-like planets (Duncan & Lissauer 1998), the decrease in the planet’s angular momentum caused by the tidal drag cannot be neglected for orbits close to the stellar radius during the AGB phase.

If the planet’s orbital distance is larger than the stellar radius reached when the star expands during the AGB phase, the variation of the orbit can be approximated by (e.g. Zahn 1977):

$$\frac{1}{r} \frac{dr}{dt} = -\frac{1}{M_*} \frac{dM_*}{dt} + \left(\frac{1}{r} \frac{dr}{dt}\right)_{tidal} \quad (1)$$

where r is the orbital distance and M_* is the stellar mass on the main sequence. The first term on the right hand side of Eq. 1 represents the increase in the orbital radius due to mass-loss from the star and the second term represents the decrease due to tidal interaction, which is proportional to $[R_*(t)/r]^8$ (Zahn 1977) and becomes negligible at large orbital distances. At small orbital distances, however, the decrease in the planet’s angular momentum caused by the tidal interaction can lead to a decrease in the orbit by ~ 100 to $300 R_\odot$ (Livio & Soker 1983; Rasio et al. 1996; Rybicki & Denis 2001), depending on the planet’s mass and the ratio of the rotational to orbital angular velocity. Note however that the stellar radius during the AGB increases gradually. Variations in the surface luminosity and radius of an AGB star arise as a consequence of the thermal and structural readjustments produced during the after-pulse phase. In particular, R_* is not maintained after a thermal-pulse. Rather, the star eventually contracts as the temperature in the He-burning shell decreases and a new thermal pulse begins.

The maximum stellar radius, R_*^{max} , is only reached briefly at the end of the AGB evolution as the star gets to the AGB tip luminosity. Consequently, it is safe to neglect the tidal term in Eq. 1 for orbital radii larger than R_*^{max} . The AGB and post-AGB evolution of the stellar mass-loss rate, effective temperature, and luminosity that we use have been obtained from the stellar evolution models of Vassiliadis & Wood (1993, 1994). From these, we have calculated the maximum radii, R_*^{max} , reached by stars of different masses during the AGB phase. These values of R_*^{max} are listed in Table 1. Neglecting tidal interaction for $r \geq R_*^{max}$ and integrating Eq. 1, the orbital radius is then given by

$$r(t) = r_o \frac{M_*}{M_*(t)} \quad (2)$$

where r_o is the initial orbital radius and $M_*(t)$ is time-dependent stellar mass caused by mass-loss.

In Fig. 1 we show the evolution of the orbital radius during the late AGB phase by using $r_o = R_*^{max}$ for each initial mass considered. In the calculation of $M_*(t)$ we have considered the fact that the AGB mass-loss accounts for most of the mass lost by low-and intermediate-mass stars and that mass-loss previous to the AGB is negligible. This is a consequence of the fact that mass-loss rates on the RGB are proportional to $R_* L_* / M_*$ (Reimers 1975), resulting in a significant amount of envelope mass lost before the AGB phase only for stars with initial masses $M_* < 1 M_\odot$.

The higher the initial mass, the higher the amount of mass lost during the AGB phase

and hence the larger the planet’s orbital expansion. Planets reach a final orbital distance at the end of the AGB phase, determined by multiplying the initial orbit by M_*/M_{WD} where M_{WD} is the white dwarf mass, given that mass-loss is negligible once the star leaves the AGB. The orbital expansion factors for each stellar mass are given in column (4) of Table 1.

Another effect to consider is whether the planet becomes unbound due to the change in mass of the central star. Unbinding can be expected if the stellar mass-loss timescale, $\tau_{mass-loss}$, satisfies $\tau_{mass-loss} < \tau_{dyn}$, where $\tau_{mass-loss}$ is given by

$$\tau_{mass-loss} \sim \frac{M_*}{\dot{M}_*} \quad (3)$$

and the dynamical timescale, τ_{dyn} , by

$$\tau_{dyn} \sim \left[\frac{r^3}{G(M_* + M_p)} \right]^{1/2}, \quad (4)$$

with \dot{M}_* being the stellar mass-loss rate, M_p the planet’s mass, and G the gravitational constant. Given that $\tau_{dyn} \sim 50$ yr while the shortest mass-loss timescale is $\tau_{mass-loss} \sim 10^5$ yr, it is very unlikely that a planet will become unbound due to the decrease in the stellar mass during the AGB phase.

A gas planet with $M_p < 15 M_J$ orbiting an AGB star (of any mass) at an initial orbital distance $r_o < R_*^{max}$ will most likely evaporate inside the stellar envelope. The deuterium burning minimum mass limit (12 M_J) is traditionally used as the mass boundary between planets and brown dwarfs (e.g. Saumon et al. 1996). Therefore we can safely state that gas planets do not survive the AGB evolution if their initial orbits lie within the reach of the stellar radius during the AGB evolution, whereas brown dwarfs can survive. For $r_o \geq R_*^{max}$ the orbit will generally expand due to the heavy stellar mass-loss rates experienced during the AGB evolution. Larger differences between the initial and final mass of the star are experienced for the more massive progenitors, causing the orbits of planets orbiting the more massive stars (note that we are always referring to stars in the 1–5 M_\odot mass range for which complete stellar evolution models exist) to be modified by the larger factors (up to 5.5 times larger than the initial orbit).

3. THE CHANGE IN THE PLANET’S ENVIRONMENT DURING THE PN PHASE

During the post-main sequence evolution of the star the stellar effective temperature always remains lower than its main sequence value. However, once the star leaves the AGB

phase, the high mass-loss rate ceases and the remnant core moves in the HR diagram at constant luminosity toward higher effective temperatures into the PN stage, before the star reaches the white dwarf cooling track. The planet’s orbit is not expected to change further at this stage. However, the main processes responsible for shaping PNe (high velocity winds) and powering PNe line emission (high stellar effective temperatures) need to be considered to establish the survival of a planet during this phase.

The luminosity, mass, and timescale of evolution of the star during the PN phase depend mostly on the stellar core mass (Paczynski 1971; Iben & Renzini 1983; Vassiliadis & Wood 1994; Iben 1995). The stellar luminosity during this phase is within the range 3.5 to $23 \times 10^3 L_{\odot}$ (for the lowest 0.56 and highest 0.9 M_{\odot} mass remnant, respectively) and the stellar temperature can reach 100 000–380 000 K (for the same core masses, respectively). The hydrogen ionizing photon flux, which is of the order of 10^{48} s^{-1} (Villaver et al. 2002b), is responsible for the PNe ionized line emission. PNe central stars also emit very high velocity winds (with speeds of a few thousands of km s^{-1}) which are driven by the transfer of photon momentum to the gas, through absorption by strong resonance lines (e.g. Pauldrach et al. 1988). The PN is largely shaped by the interaction of this high velocity wind with the slowly ejected material during the AGB phase (Kwok et al. 1978; Kahn & West 1985; Balick 1987; Mellema & Frank 1995; Villaver et al. 2002a,b). The survival of a gas planet as the star evolves into the PN phase strongly depends on the planet’s surface temperature, which ultimately determines whether or not high evaporation rates are set at the planet’s surface.

3.1. The Planet’s Equilibrium Temperature

The radiative equilibrium temperature of a planet can be estimated by balancing the flux received by the star to the blackbody flux re-radiated by the planet,

$$\sigma T_p^4 = \frac{L_*}{16\pi r^2}(1 - A) \quad (5)$$

where σ is Steffan-Boltzmann’s constant, T_p is the planet’s equilibrium temperature, r is the orbital radius, L_* is the stellar luminosity and A is the Bond albedo. We have assumed an approximate value of $A = 0.5$. As shown in Marley et al. (1999) Bond albedos show little sensitivity to the planet’s gravity or effective temperature for a given stellar spectrum; the largest variations arise from the stellar spectral type and the presence of clouds.

Fig. 2 shows the planet’s equilibrium temperature versus orbital distance as given by Eq. 5 for the two extreme cases of primaries: the lowest and the highest stellar masses considered. Internal energy sources have not been considered in Eq. 5 since they are expected

to be negligible.

A planet orbiting a PN central star will have an age in the range 0.1 to 10 Gyr as the star enters the PN phase, assuming that the star and the planet are coeval. Burrows et al. (2001) and Hubbard et al. (2002) show the predicted range of effective temperatures for *isolated* giant planets and brown dwarfs of various masses to be between 100 K and 400 K for the age range of interest here. The cooling theory applies equally to the structure and evolution of brown dwarfs and giant planets, given their convective nature. From Fig. 2 we see that the planet’s equilibrium temperature in the presence of the PN core is much higher than the expected value in isolation, at orbital distances $r \leq 20$ AU and $r \leq 50$ AU for the 0.56 and 0.9 M_{\odot} stars respectively.

3.2. The Planet’s Exospheric Temperature

Given the high effective temperature of the star, most of the stellar flux is emitted at short wavelengths, for which the material in the planet’s atmosphere has a high optical depth. The incident flux will therefore be absorbed by a thin surface layer, the depth of which will be determined by the transparency of the material to the incident photons. Inward to this surface layer, the heat transfer to the interior is set by a combination of conduction and convection. The temperature on the planet’s atmosphere has to be determined through the energy equation considering radiative, conductive and convective terms. Convective effects are expected to be important in the atmosphere of a tidally synchronized planet, since a strong temperature gradient will be set between the day and night side of the planet. However, only very short period planets are expected to be tidally synchronized (Guillot et al. 1996) and planets orbiting PN central stars are not expected to be found at such short orbital periods (see §2). Therefore, it is reasonable to assume that, for the case under consideration, convection can be neglected as first approximation. Moreover, it has been shown that in the upper atmosphere of a planet (the exosphere) the density becomes very low and the temperature is determined mainly by the absorption of extreme ultraviolet and X-ray (XUV) radiation (Bauer & Lammer 2004). Therefore by neglecting convective effects the energy equation takes the simplified form:

$$\nabla \cdot (K \nabla T - q_{\text{xuv}}) = 0 \tag{6}$$

where q_{xuv} is the effective radiative heat flux of the star at wavelengths shorter than 3000 Å for which the opacity is very high, T is the temperature, and K is the thermal conductivity. The exospheric temperature, T_{ex} , can be obtained by integrating Eq. 6. This gives (see e.g.

Bauer 1971, 1973),

$$T_{ex}^{s+1} - T_b^{s+1} \simeq \frac{\alpha k_b \sigma_c \epsilon I_\infty}{K_o m_H g \sigma_a} T_{ex} \quad (7)$$

where s is the temperature dependence of the thermal conductivity, $s = 0.7$ for atomic hydrogen (Dalgarno & Smith 1962), T_b is the temperature at the base of the thermosphere, α is a factor that takes into account the rotation of the planet and varies between 0.5 and 0.25 for rapid or slow rotators, k_b is Boltzman’s constant, σ_c is the gas-kinetic collision cross-section, K_o is the thermal conductivity proportionality factor, m_H the mass of the hydrogen atom, and g is the gravitational acceleration. The intensity of the stellar radiation reaching the planet’s atmosphere I_∞ is related to q_{xuv} by,

$$q_{xuv} = n_j \sigma_a \epsilon I_\infty e^{-\tau} \quad (8)$$

where ϵ is the heating efficiency (the fraction of the stellar flux absorbed that is transformed into thermal energy in the atmosphere), and τ is the optical depth, with $\tau = \int n_j \sigma_a dz$ where n_j is the number density of the absorbing constituent (atomic hydrogen), σ_a its absorption cross section to XUV radiation and z is the atmospheric altitude.

Since T_b is roughly equal to the planet’s equilibrium temperature, then $T_b \ll T_{ex}$ and the second term on the left hand side of Eq. 7 can be neglected. Note that in order to estimate T_{ex} in Eq. 7 cooling in the infrared has not been considered. This is justified by the fact that most of the molecular hydrogen (which is responsible for the cooling in the infrared) is expected to be dissociated in the upper atmosphere.

In Fig. 3 we show the exospheric temperature T_{ex} reached by a Jupiter-like planet of 1 M_J mass due to the XUV generated by a 0.56 M_\odot (1 M_\odot main sequence mass) central star versus the orbital distance. The different curves are the result of changing the XUV flux intensity due to the evolution of the star in the HR diagram. The stellar luminosity emitted below 3000Å has been estimated using the GMFGEN code of Hillier & Miller (1998, 1999). Note that for a PN central star with an effective temperature of 115 000 K (and $\log g = 5.7$), 97 % of the total stellar luminosity is emitted below 3000 Å. For cooler central stars (e.g. 35 000 K), 93% of the stellar luminosity is below 3000 Å. The solid curve represents T_{ex} obtained by using the stellar flux early in the evolution of the star into the PN phase when the stellar luminosity is $L_* = 3600 L_\odot$ and $T_{eff} = 36000$ K; the dashed curve corresponds to an intermediate stage ($L_* = 1400 L_\odot$ and $T_{eff} = 115000$ K); and the dotted curve corresponds to a point 10^5 yr later in the evolution, when the luminosity has dropped to $100 L_\odot$ at a temperature of $T_{eff} = 96000$ K. In the following, we explore the conditions under which an evaporation flow is established at the planet’s surface.

4. PLANET EVAPORATION DUE TO THERMAL HEATING DURING THE PN PHASE

The standard formulation for the gas-kinetic or thermal evaporation from celestial bodies was first established by Jeans (1925). Jeans’s formula gives a lower limit to the rate of escape (by thermal evaporation) of gas from a planetary atmosphere:

$$\Phi_J = \frac{v_o}{2\sqrt{\pi}} n_c (1 + E) e^{-E} \quad (9)$$

where $v_o = \sqrt{2k_b T/m_H}$ is the velocity of the escaping particles, n_c is the number density of the escaping constituent (we assume hydrogen from now onwards) at a given critical level, T is the temperature, and E is the escape parameter $E(R) = GMm_H/Rk_bT$ where M is the planet’s mass contained within a spherical surface of radius R , and k_b and G are Boltzman’s and the gravitational constants respectively. *Jeans escape* then usually refers to the density of the critical level n_c at the exobase, that delineates the lower limit of the exosphere (e. g. Chamberlain & Hunten 1987). The temperature of this layer, the exospheric temperature T_{ex} , is much higher than the planet’s effective temperature (given by Eq. 5), and higher than the gas photoionization temperature (10 000 K) and is the characteristic planetary temperature for thermal escape (Moutou et al. 2001; Lammer et al. 2003; Baraffe et al. 2004; Lecavelier des Etangs et al. 2004). A common misconception when considering the evolution of a planet inside a PN, is that the evaporation rates are determined by the Jeans escape, with a temperature of 10 000 K fixed by photoionization. Using the ionization temperature the sound speed of the ionized gas in the planet’s atmosphere is smaller than the typical escape velocity for the material and therefore no evaporation is expected.

Equation 9 seems to imply that high evaporation rates may be achieved for high values of n_c . However, *Jeans escape* is only valid when the escape rate is relatively small and therefore the static structure of the atmosphere is not perturbed, that is, when the escape parameter $E \geq 20$ -30. Note that E represents the ratio of the gravitational potential energy to the particle kinetic energy or, in other words, the ratio of the square of the escape to the thermal velocity in the upper atmosphere. For large escape fluxes, $E \leq 20$, the structure of the upper atmosphere is modified, the gas that has escaped has to be replaced by gas from the lower levels thereby altering the atmospheric structure. In this case, the escape rate given by Eq. 9, and the thermal balance are no longer valid (Chamberlain & Hunten 1987; Bauer & Lammer 2004). For $E \leq E_c$, where $E_c \approx 1.5 - 3$, the atmosphere reaches blow-off conditions (e.g. Öpik 1963). The exospheric base is lifted outwards, the planet radius increases and the atmosphere is lost if the heat source continues to operate. Under blow-off conditions the planet’s atmosphere will expand radially outward at relatively modest,

subsonic velocities, close to the surface, and will gradually accelerate to supersonic velocities as it moves further away. Fig. 3 shows that blow-off conditions (represented by the region above the solid or the dotted horizontal line depending on the E_c value assumed) are easily reached at the planetary atmosphere up to distances of 125 AU.

As the stellar mass is increased, higher luminosities and effective temperatures than the ones used in Fig. 3 are reached during the PN phase. More intense XUV radiation fields will reach a planet’s atmosphere orbiting a higher mass progenitor. The results shown in Fig. 3 therefore represent a lower limit (in stellar mass) to the development of blow-off conditions. Although we have assumed a hydrogen composition to compute T_{ex} , if other, heavier constituents exist they will be carried away through drag forces (by the light gas moving at a sonic speed) once the atmosphere reaches the blow-off condition.

The escape parameter, as well as the exospheric temperature, depend on the planet’s surface gravity. The higher the planet’s mass, the harder it is to reach the blow-off conditions because the particles need a much higher thermal energy to reach escape velocities at the planet’s surface. The gray area in Fig. 4 shows the orbital distance region (to 125 AU) at which a planet’s or a brown dwarf’s atmosphere will reach blow-off conditions as a function of the planet (or brown dwarf) mass. In the calculation we have used mass-radius relations given by Baraffe et al. (2003) for non-irradiated extrasolar planets at 10 Gyr, and assumed that the exospheric temperature is given by Eq. 7. The left and right panels have been computed for a $0.56 M_{\odot}$ ($1 M_{\odot}$ main sequence) and $0.9 M_{\odot}$ ($5 M_{\odot}$ main sequence) star respectively, early in the PN phase. We have chosen the same effective temperature of the star, 36 000 K, which corresponds to $L_* = 3\,600 L_{\odot}$ and $L_* = 23\,000 L_{\odot}$ respectively. Higher mass stars produce more intense XUV radiation fields and blow off conditions are set at larger orbital distances for a given planet mass. The evolution of the star towards higher effective temperatures has similar effects.

4.1. The Planet’s Evaporation Rates

Given the high exospheric temperatures reached at the planet’s upper atmosphere it is expected that an outflow will develop as a consequence of the absorption of the XUV radiation. Since high temperatures can cause the outer layers of the planet to escape rapidly, in order to examine the planet survival, we have to estimate the evaporation rate. Note that at the orbital distances we are considering, the planet will be well within the typical inner radius of the nebular shell (0.01 to 0.1 pc) (Villaver et al. 2002b), so we do not expect a decrease in the photon flux arriving at the planet’s surface due to absorption by the nebula.

The problem of a general outflow from a stellar (or planetary) body can be described with the same set of equations used by Parker (1963) to describe the solar wind. Although a complete treatment of the evaporative wind requires the integration of the energy, mass, and momentum transfer equations, we can estimate the outflowing particle flux Φ_H (e.g. Watson et al. 1981) by equating the energy input $(\epsilon L_{\text{xuv}}/4) \times (R_1/r)^2$ to the energy required for hydrogen to escape $GM_p m_H/R_p$, giving

$$\Phi_H \simeq \frac{\epsilon L_{\text{xuv}} R_1^2 R_p}{4r^2 GM_p m_H} \quad (10)$$

where R_1 is the planet’s radius where most of the XUV radiation is absorbed, defined as the level where the optical depth is unity, r is the orbital distance, R_p and M_p are the planet’s radius and mass respectively and ϵL_{xuv} the fraction of the stellar XUV luminosity (see §3.2) that is converted into thermal energy. A proper determination of ϵ requires the solution of the atmospheric structure (Yelle 2004). Most calculations in the literature assumed the value of $\epsilon = 0.63$ determined for Jupiter by Waite et al. (1983) (e.g. Yelle (2004)). Note, however, that Cecchi-Pestellini et al. (2006) have recently estimated the X-ray contribution to exospheric heating in hydrogen-rich planetary atmospheres and found heating rates significantly higher than those used by Yelle (2004) for planets at the same distance from the central star. Given the high effective temperatures reached by PN central stars we consider it reasonable to assume a value of $\epsilon = 1$.

The determination of R_1 , or $\xi = R_1/R_p$, is not an easy task, as it requires the full solution of the hydrodynamical escape problem with radiation transfer in a strongly externally heated atmosphere. Watson et al. (1981) assumed a single layer atmosphere and an iterative method to solve the problem. Lammer et al. (2003) and Baraffe et al. (2004) used Watson’s solution for R_1 which matched the observed expanded atmosphere of HD 209458b ($R_1 = 3 R_J$). Note that in this approach it is implicitly assumed that R_1 lies below the *sonic level*.

Lower mass-loss rates (by a factor of 20) than those estimated under hydrodynamical blow-off for HD209458b, have been obtained by Lecavelier des Etangs et al. (2004), by using what they refer to as *geometrical blow-off*: a combination of Jeans escape rates and tidal forces. Under geometrical blow-off the high exospheric temperatures push the position of the exosphere to the Roche-lobe limit before hydrodynamical blow-off (or energy-limited mass-loss) conditions develop, resulting in lower mass-loss rates than those estimated under hydrodynamical blow-off. Tian et al. (2005) found an escape rate 16 times smaller (for a heating efficiency of 0.6) than the maximum evaporation rate derived by Lammer et al. (2003) and Baraffe et al. (2004) for HD 209458b and consistent with that determined by Lecavelier des Etangs et al. (2004). More recently, Jaritz et al. (2005) have shown that exoplanets at small orbital distances will be subjected to either hydrodynamical or geometrical

blow-off conditions depending on where the position of the exobase reaches the Roche lobe limit.

In the Tian et al. (2005) simulation the hydrodynamical escape of hydrogen from a planetary atmosphere was studied by allowing transonic solutions and using a two dimensional energy deposition layer. With this approach they found the escape rates to depend on the position of the heating layer as well as on the amount of energy input, with the escape rate exponentially increasing with the heating rate. Tian et al. (2005) also found Watson’s escape fluxes to be too high when low density hydrogen atmospheres are involved (as in the case HD 209458b). At hydrogen number densities higher than 10^{14} cm^{-3} , Tian et al. (2005) find higher escape rates than Watson. Generally, the simulations produce higher escape rates than the ones given by Eq. 10 for $\xi = 3$ as the density increases. This is the result of the higher total amount of energy absorbed in an extended atmosphere, as opposed to that absorbed in a single layer (the approximation used to obtain Eq. 10).

The mass-loss rates (obtained by using $\xi = 3$ in Eq. 10) from a $1 M_J$ planet for central stars (at 36 000 K) with different masses are plotted in Fig. 5, versus the orbital distance. Note that the value of ξ used in Fig. 5 is always smaller than that obtained by Erkaev et al. (2006) for the exoplanets in which the mass, radius and stellar parameters are known. The different lines account for the different central star masses considered, with the mass-loss rates increasing with the stellar mass.

It is important to note that for the *geometrical blow-off* (Lecavelier des Etangs et al. 2004) to operate, the planet has to be in a very close orbit to the parent star which is never the case for planets to be found around PN central stars. Moreover, none of the calculations in the literature includes heating rates as high as the ones expected for a planet orbiting a PN central star, and as it has been shown by Cecchi-Pestellini et al. (2006), the inclusion of X-ray irradiation from the star strongly increases the heating in planetary exospheres. Therefore, the mass-loss rates given in Fig. 5 should be considered merely as order of magnitude approximations to the actual mass-loss rates from a planet exposed to a PN central star. In addition, it is very likely that the planet will inflate as radiation is transformed into heat inside its atmosphere, which will lead to further increase in the planet’s evaporation rate with our approach. An appropriate determination of the escape rate will require a solution of the hydrodynamic escape equations for the case under consideration.

5. THE PLANET EVOLUTION UNDER MASS-LOSS

Central stars of PN do not maintain high luminosities for an extended period of time and therefore the evaporation rates shown in Fig. 5 will change as the star evolves. In Fig. 6 we show the evolution of the evaporation rate of a $1M_J$ planet orbiting a $0.56 M_\odot$ PN central star at two orbital distances: 1.5 AU and 5 AU (solid and dashed lines respectively). The evaporation rate has been computed using $\xi = 3$ in Eq. 10 and the evolution of the stellar flux from the models of Vassiliadis & Wood (1994) extended to the white dwarf cooling tracks using the Prada Moroni & Straniero (2002) models.

It is important to note that the evolution of the evaporation rate shown in Fig. 6 is clearly an oversimplification of the real case, which involves factors other than the evolution of the stellar luminosity. For instance, feedback processes are important because the evaporation rate depends on the planet’s structure which is itself determined by the planet’s reaction to evaporation and heating. In order to establish the importance of the feedback processes in determining the evaporation rates we need an estimate of the relevant timescales. The timescale over which significant reaction takes place is given by the thermal timescale τ_{th} . For the case under consideration the heating by radiation is taking place in a thin layer near the surface of the planet where the opacity is very high. Therefore, the relevant thermal timescale is the one associated to the heating of the planet’s external layer by an external heating source, $\tau_{\text{th}} = GM_p \Delta M / 2RL_*$, where ΔM is the mass that is being heated and L_* is the stellar luminosity arriving at the planet’s surface (multiplied by a correction factor that accounts for the heating efficiency). Since Jupiter-like planets are believed to be mostly convective, with a radiative external zone that contains $\approx 0.03\%$ of the mass (Guillot et al. 1996), it is reasonable to assume that the stellar energy is mostly deposited in this layer, which then gives $\tau_{\text{th}} \approx 10^6$ yr (for a $0.56 M_\odot$ star). We should now compare τ_{th} with the mass-loss timescale $\tau_{\dot{M}}$, $\tau_{\dot{M}} = M_p / \dot{M}_p$, and if we assume that $\dot{M}_p = \Phi_H$ as given by Eq. 10 then $\tau_{\dot{M}} \approx 10^5$ yr (for $1 M_J$ and $0.56 M_\odot$). Therefore, for range of orbital distances, $\tau_{\dot{M}} \leq \tau_{\text{th}}$ which implies that the planet’s mass is decreasing faster than the time the planet has to readjust to a new thermal equilibrium.

The planet has two ways to adjust to a new thermal equilibrium: to increase its radius or to increase its effective temperature. If the planet reacts to the external heating by increasing its effective temperature, then the evolution of the mass-loss rates computed using Eq. 10 and the time-dependent stellar flux are a good first order approximation to the actual evaporation rates. However, given the high mass-loss rates involved, the planet may react by increasing its radius on a timescale given by τ_{th} , in which case the mass-loss rates will be larger than estimated. In fact, once the mass-loss timescale becomes much shorter than the readjustment (thermal) timescale ($\tau_{\dot{M}} \lesssim 0.1\tau_{\text{th}}$), a runaway mass-loss may ensue

(e.g. Baraffe et al. 2003).

5.1. Other Evaporative Processes

There are other non-thermal processes that might contribute to the planet evaporation, e.g. photodissociation and ram pressure stripping. An increase in the planet’s radius will decrease the density of the outer layer allowing the ionization front to propagate inwards, deeper into the structure of the planet. It can be easily shown that given the high densities involved, photoionization in itself cannot destroy a Jupiter-like planet. However, the ionization of the gas increases the pressure (as it increases the number of particles and the temperature), causing an expansion of the outer layers that is driven from the outside and not from the luminosity of the planet’s interior. It has even been suggested that a Jupiter like planet could be detected by the variable hydrogen recombination line emission it would emit in its outer atmosphere which is photoionized by the PN central star (Chu et al. 2001).

Ram pressure stripping caused by the stellar wind might become a very efficient process in removing mass from the outer layers, once the planet expands. Ram pressure stripping could dominate during the early stages of the evolution of the PN phase, when high velocity winds (with still relatively high densities) directly impact the planet’s surface (at that stage $\rho_w v_w^2|_{star} > (\dot{M}_p/4\pi R_p^2)v_e|_{planet}$ with v_e the planet’s escape velocity). Ram pressure stripping due to the stellar proper motion has been shown to be a very efficient process in removing mass from PN shells (Villaver et al. 2003; Villaver & Stanghellini 2005). Furthermore, evaporation rates might increase significantly when one takes into account the rotation of the planet (Burke 1969).

As the star evolves, the wind velocity increases, reaching a velocity above which the shocked gas is not able to cool down radiatively. An adiabatic shock then develops at the interaction region between the high-velocity stellar wind and the dense material ejected previously during the AGB, forming what is known as the hot bubble. The post-shocked gas temperature can easily reach 10^6 – 10^7 K and has been observationally confirmed through the detection of diffuse extended X-ray emission (Chu et al. 2001; Guerrero et al. 2002, 2005). The outer radius of the hot bubble can reach ~ 0.1 pc and the reverse shock region is expected to be very close to the star (Villaver et al. 2002b). Therefore, the planet’s orbit will be immersed inside an environment at the hot bubble temperature of 10^6 - 10^7 K. The hot bubble, however, does not develop immediately (Villaver et al. 2002b), because the wind velocity needs to be high enough to develop an adiabatic shock. It is then expected that the temperature of the planet’s atmosphere will be first set by the absorption of XUV radiation as described in §3.2, and only during later stages of the star’s evolution the hot bubble will

provide an additional heating source.

It can be expected that photoionization, ram pressure stripping and the presence of the hot bubble will increase the evaporation rate from a gas planet orbiting a PN central star. All these processes have not been included in the evaporation rates given in Fig. 5 (for $\xi = 3$ which should therefore be regarded as representing conservative lower limits.

6. PLANET SURVIVAL

We have shown that for small orbital distances the planet’s structure will change on timescales longer than the mass-loss timescales and that the most likely response will be an increase in the planet’s radius. As a first approximation and since we are not computing the rate of change of the planet’s radius (a problem that requires a full hydrodynamic calculation) we have estimated the planet’s survival by integrating the evaporation rates obtained by evolving the stellar flux under different assumptions for ξ . As mentioned in §4.1, $\xi=3$ represents the most conservative scenario, most likely a lower limit to the evaporation rate of the planet. Note that for this particular problem, an increase in the planet’s radius will naturally lead to lower densities in the outer layer, making the planet more vulnerable to the erosion caused by photoionization and ram pressure stripping. Since we have not quantified all these effects when estimating the evaporation rates in Eq. 10, using $\xi=10$ is probably a reasonable assumption. Note that Tian et al. (2005) have shown that the position of the exobase for the extended atmosphere of HD 209458b is close to $\xi = 10$.

Table 2 lists the percentage of the planet that is evaporated until a $0.56 M_{\odot}$ star enters the white dwarf cooling track. Column (1) gives the initial planet mass, column (2) the orbital radius, and columns (3), (4) and (5) give the percentage of the planet mass evaporated by using $\xi=3$, 5, and 10 respectively. Note that although we have extended the evolutionary time into the white dwarf cooling sequence, most of the planet’s evaporation takes place as the star is evolving during the PN phase.

In Fig. 7 we show the region (on the planet mass versus orbital distance plane) inside which Jupiter-like planets will be destroyed, as the star evolves off the main sequence. The left and right panels are for planets orbiting a 0.56 and $0.9 M_{\odot}$ star respectively (which correspond to 1 and $5 M_{\odot}$ main sequence masses). The light gray area represents the region inside which the planet will be engulfed and most likely destroyed as the star ascends the AGB. The dark gray and shaded areas (computed for $\xi=3$ and 10 respectively) represent the regions for which planets will lose 50 % of their mass before the star enters the white dwarf cooling track due to the evaporation caused by thermal heating. Note that the region for

which the planet will undergo total evaporation due to thermal heating is inside the AGB stellar radius for the $0.9 M_{\odot}$ star.

Giant planets are thought to be formed in cool regions of the protoplanetary disk—beyond the ice line—where there is enough solid material to produce a core that will capture the gas (Sasselov & Lecar 2000; Kornet et al. 2004). Planet migration (e.g. Trilling et al. 1998; Armitage et al. 2002) is then used in order to explain the close distances at which such planets are observed around sun-like stars (e.g. Mayor & Queloz 1995; Vidal-Madjar et al. 2004; Marcy et al. 2005). Most of the planets recently discovered are giant planets orbiting sun-like stars at orbits ≤ 5 AU.

The conditions for planet survival as the star evolves off the main sequence depend on the initial mass of the star. From Fig. 7 we see that most of the close-in planets ($r \leq 1.5$ AU) will be destroyed as they get engulfed by the star during the AGB phase (see Table 1 for a list of the maximum stellar radius reached during the AGB versus the stellar mass). As the star leaves the AGB and enters the PN phase, high effective temperatures at very high luminosities set up an evaporation flux at the surface of the planet. At certain orbital distances the evaporation rates are high enough to cause a total destruction of the planet. By integrating the evaporation rates as the star evolves during the PN into the white dwarf cooling track, we find that Jupiter-like planets will be destroyed if they remain at orbital distances $r \leq 5$ AU from a low mass white dwarf ($M_{\text{WD}} \leq 0.63 M_{\odot}$) and large planet ablation is expected up to 10 AU. In particular, Jupiter in our own Solar system is barely expected to survive. More massive stars evolve very fast during the PN phase and do not maintain high evaporation rates long enough to cause planet destruction, unless the planets were to be found at small orbital distances ($r \leq 2.5$ AU). However, we have shown that planets orbiting the more massive PN central stars cannot be found at small orbital distances: if a planet orbiting a $0.9 M_{\odot}$ progenitor is to survive AGB engulfment then its orbit has to be at $r \geq 29$ AU.

Over the last few years several groups have surveyed white dwarfs in the search for planets with no positive results reported so far. The wide field proper motion survey around 261 white dwarfs by Farihi et al. (2005) was sensitive to 100 to 5000 AU with masses down to $52 M_{\text{J}}$, and their deeper near field search of 86 white dwarfs could detect $10 M_{\text{J}}$ at separations between 50 and 1100 AU. Mullally et al. (2006) have recently surveyed 124 white dwarfs with Spitzer and found no evidence for planets with $M \geq 5 M_{\text{J}}$. Using direct imaging Zinnecker et al. (2006) have ruled out the presence of giant planets ($6\text{-}12 M_{\text{J}}$) around the 7 known white dwarfs of the Hyades cluster. A planet ($4 M_{\text{J}}$) was discovered in the binary system Gliese 86 by Mugrauer & Neuhäuser (2005) orbiting the K1 dwarf in Gliese 86A, which has a $0.55 M_{\odot}$ mass white dwarf companion, Gliese 86B, at 21 AU. At this distance

from the white dwarf, we expect the planet to have been losing mass during the PN phase at such a low rate that it would not have affected its survival.

On the other hand, three white dwarfs are known to possess an infrared excess, GD 362 (Zuckerman & Becklin 1987; Becklin et al. 2005; Kilic et al. 2005), G29-39 (Jura 2003) and the recently discovered GD 56 (Kilic et al. 2006). To explain G 29-38 Jura (2003) proposed a disk formed by the tidal destruction of an asteroid. The destruction and accretion of a planetary body continues to be the widely accepted scenario to explain the high anomalous photospheric abundances in the massive white dwarf GD 362, where a massive accretion disk has been detected (Becklin et al. 2005; Kilic et al. 2005). We have shown that planets around the most massive white dwarfs are expected to be found at $r \geq 30$ AU, due to the expansion of the planetary orbit during AGB mass-loss. How a planet at such a large distance from the star would then be disrupted (in order to form an accretion disk) is by no means clear. Another more plausible scenario for the presence of accretion disks around massive white dwarfs, is that they are formed by the merger of two white dwarfs (Livio et al. 2005), a scenario that can also explain the presence of planets around massive white dwarfs at small orbital distances.

7. CONCLUSIONS

Planets at orbital distances within the reach of the stellar radius during the AGB phase will spiral-in and totally evaporate. The AGB stellar radius depends on the stellar mass and therefore so does the distance from the parent star at which a planet is destroyed, $r \leq 1.6$ AU for $M_* = 0.56 M_\odot$ and $r \leq 5.3$ AU for $M_* = 0.9 M_\odot$.

If the planet avoids engulfment its orbit will typically expand. The final masses of white dwarfs are primarily established during the AGB phase due to heavy mass-loss. The more massive progenitors (when on the main sequence) lose larger amounts of mass during the AGB, thus the planets orbiting these stars will experience the largest orbital readjustments.

We show that as the star evolves into the PN phase, high temperatures are reached in the outer atmosphere of the planet resulting in the development of blow-off conditions. As the star evolves through the PN phase into the white dwarf cooling track:

1. An general outflow is established at the surface of a substellar object. The evaporation flux decreases with the orbital distance, and as the star evolves, with higher evaporation fluxes expected for planets orbiting the more massive stars. The evaporation rates are sufficiently high ($10^{-5} M_J \text{yr}^{-1}$ at 5 AU for a $1M_J$ planet) that these evaporating planets

may be detected using spectroscopic observations, similar to those performed for HD 209458b by Vidal-Madjar et al. (2003).

2. Under these evaporation rates, planets with $M_p \leq 1 M_J$ will not survive the PN phase if located at orbital distances $r \leq (3-5)$ AU.
3. Planets with $M_p > 2M_J$ survive the PN phase down to orbital distances of ~ 3 AU around low-mass ($M_{WD} \sim 0.56 M_\odot$) central stars.
4. Planets around white dwarfs with masses $M_{WD} \gtrsim 0.7 M_\odot$ (that formed from single stars with masses $M_{MS} \gtrsim 2.5 M_\odot$), are generally expected to be found at orbital radii $r \gtrsim 15$ AU due to the effects of mass-loss on the AGB phase. If planets are found at smaller orbital radii around such massive white dwarfs, they had to form as a result of the merger of two white dwarfs (Livio et al. 2005).

Acknowledgment: We are grateful to James Herald for providing us with the stellar fluxes from the CMFGEN code.

REFERENCES

- Armitage, P. J., Livio, M., Lubow, S. H., & Pringle, J. E. 2002, MNRAS, 334, 248
- Bauer, S. J. 1971, Nature, 232, 101
- Bauer, S. J. 1973, Physics of Planetary ionospheres (Heildeberg: Springer)
- Bauer, S. J., & Lammer, H. 2004, Planetary aeronomy : atmosphere environments in planetary systems. Berlin: Springer, 2004.
- Balick, B. 1987, AJ, 94, 671
- Baraffe, I., Chabrier, G., Barman, T. S., Allard, F., & Hauschildt, P. H. 2003, A&A, 402, 701
- Baraffe, I., Selsis, F., Chabrier, G., Barman, T. S., Allard, F., Hauschildt, P. H., & Lammer, H. 2004, A&A, 419, L13
- Becklin, E. E., Farihi, J., Jura, M., Song, I., Weinberger, A. J., & Zuckerman, B. 2005, ApJ, 632, L119
- Burleigh, M. R., Clarke, F. J., & Hodgkin, S. T. 2002, MNRAS, 331, L41

- Burrows, A., et al. 1997, *ApJ*, 491, 856
- Burrows, A., Hubbard, W. B., Lunine, J. I., & Liebert, J. 2001, *Reviews of Modern Physics*, 73, 719
- Cecchi-Pestellini, C., Ciaravella, A., & Micela, G. 2006, *A&A*, 458, L13
- Hubbard, W. B., Burrows, A., & Lunine, J. I. 2002, *ARA&A*, 40, 103
- Burke, J. A. 1969, *MNRAS*, 145, 487
- Chamberlain, J. W., & Hunten, D. M. 1987, *Theory of Planetary Atmospheres* (Orlando FL Academic Press Inc International Geophysics Series)
- Chu, Y.-H., Dunne, B. C., Gruendl, R. A., & Brandner, W. 2001, *ApJ*, 546, L61
- Chu, Y.-H., Guerrero, M. A., Gruendl, R. A., Williams, R. M., & Kaler, J. B. 2001, *ApJ*, 553, L69
- Dalgarno, A., & Smith, F. J. 1962, *Planet. Space Sci.*, 9, 1
- Debes, J. H., & Sigurdsson, S. 2002, *ApJ*, 572, 556
- Debes, J. H., Sigurdsson, S., & Woodgate, B. E. 2005, *AJ*, 130, 1221
- Duncan, M. J., & Lissauer, J. J. 1998, *Icarus*, 134, 303
- Erkaev, N. V., Lammer, H., Kulikov, Y. N., Langmayr, D., Selsis, F., Jaritz, G. F., & Biernat, H. K. 2006, *ArXiv Astrophysics e-prints*, arXiv:astro-ph/0612729
- Farihi, J., Becklin, E. E., & Zuckerman, B. 2005, *ApJS*, 161, 394
- Friedrich, S., Zinnecker, H., Brandner, W., Correia, S., & McCaughrean, M. 2005, *ASP Conf. Ser.* 334: 14th European Workshop on White Dwarfs, 334, 431
- Guerrero, M. A., Gruendl, R. A., & Chu, Y.-H. 2002, *A&A*, 387, L1
- Guerrero, M. A., Chu, Y.-H., Gruendl, R. A., & Meixner, M. 2005, *A&A*, 430, L69
- Guillot, T., Burrows, A., Hubbard, W. B., Lunine, J. I., & Saumon, D. 1996, *ApJ*, 459, L35
- Hillier, D. J., & Miller, D. L. 1998, *ApJ*, 496, 407
- Hillier, D. J., & Miller, D. L. 1999, *ApJ*, 519, 354
- Iben, I., Jr., & Renzini, A. 1983, *ARA&A*, 21, 271

- Iben, I. 1995, *Phys. Rep.*, 250, 2
- Ignace, R. 2001, *PASP*, 113, 1227
- Jaritz, G. F., Endler, S., Langmayr, D., Lammer, H., Grießmeier, J.-M., Erkaev, N. V., & Biernat, H. K. 2005, *A&A*, 439, 771
- Jeans, S. J. 1925 in *The dynamical theory of gases*. Cambridge: University Press; (4th edition, Dover Publications, N. Y.)
- Jura, M. 2003, *ApJ*, 584, L91
- Kahn, F. D., & West, K. A. 1985, *MNRAS*, 212, 837
- Kilic, M., von Hippel, T., Leggett, S. K., & Winget, D. E. 2005, *ApJ*, 632, L115
- Kilic, M., von Hippel, T., Leggett, S. K., & Winget, D. E. 2006, *ApJ*, 646, 474
- Kwok, S., Purton, C. R., & Fitzgerald, P. M. 1978, *ApJ*, 219, L125
- Kornet, K., Różyczka, M., & Stepinski, T. F. 2004, *A&A*, 417, 151
- Lecavelier des Etangs, A., Vidal-Madjar, A., McConnell, J. C., & Hébrard, G. 2004, *A&A*, 418, L1
- Lammer, H., Selsis, F., Ribas, I., Guinan, E. F., Bauer, S. J., & Weiss, W. W. 2003, *ApJ*, 598, L121
- Livio, M., & Soker, N. 1983, *A&A*, 125, L12
- Livio, M., & Soker, N. 1984, *MNRAS*, 208, 763
- Livio, M., Pringle, J. E., & Wood, K. 2005, *ApJ*, 632, L37
- Marcy, G. W., Butler, R. P., Vogt, S. S., Fischer, D. A., Henry, G. W., Laughlin, G., Wright, J. T., & Johnson, J. A. 2005, *ApJ*, 619, 570
- Marley, M. S., Gelino, C., Stephens, D., Lunine, J. I., & Freedman, R. 1999, *ApJ*, 513, 879
- Maxted, P. F. L., Napiwotzki, R., Dobbie, P. D., & Burleigh, M. R. 2006, *Nature*, 442, 543
- Mayor, M., & Queloz, D. 1995, *Nature*, 378, 355
- Mellema, G., & Frank, A. 1995, *MNRAS*, 273, 401

- Moutou, C., Coustenis, A., Schneider, J., St Gilles, R., Mayor, M., Queloz, D., & Kaufer, A. 2001, *A&A*, 371, 260
- Mugrauer, M., & Neuhäuser, R. 2005, *MNRAS*, 361, L15
- Mullally, F., Winget, D. E., & Kepler, S. O. 2006, *ASP Conf. Ser. 352: New Horizons in Astronomy: Frank N. Bash Symposium*, 352, 265
- Nelemans, G., & Tauris, T. M. 1998, *A&A*, 335, L85
- Öpik, E. J. 1963 Selective scape of gases. *Geophys. J. Roy. Astron. Soc.*, 7, 490-509
- Paczynski, B. 1971, *Acta Astronomica*, 21, 417
- Parker, E. N. 1963, *Interplanetary Dynamical Processes*, New York, Wiley, 51-91
- Pauldrach, A., Puls, J., Kudritzki, R. P., Mendez, R. H., & Heap, S. R. 1988, *A&A*, 207, 123
- Portegies Zwart, S. F., & Yungelson, L. R. 1998, *A&A*, 332, 173
- Prada Moroni, P. G., & Straniero, O. 2002, *ApJ*, 581, 585
- Rasio, F. A., Tout, C. A., Lubow, S. H., & Livio, M. 1996, *ApJ*, 470, 1187
- Reimers, D. 1975, *Problems in stellar atmospheres and envelopes.*, 229
- Rybicki, K. R., & Denis, C. 2001, *Icarus*, 151, 130
- Sackmann, I.-J., Boothroyd, A. I., & Kraemer, K. E. 1993, *ApJ*, 418, 457
- Saumon, D., Hubbard, W. B., Burrows, A., Guillot, T., Lunine, J. I., & Chabrier, G. 1996, *ApJ*, 460, 993
- Siess, L., & Livio, M. 1999, *MNRAS*, 304, 925
- Siess, L., & Livio, M. 1999, *MNRAS*, 308, 1133
- Soker, N. 1994, *PASP*, 106, 59
- Soker, N. 1996, *ApJ*, 460, L53
- Soker, N. 1998, *AJ*, 116, 1308
- Struck, C., Cohanin, B. E., & Willson, L. A. 2002, *ApJ*, 572, L83

- Struck, C., Cohanin, B. E., & Willson, L. A. 2004, *MNRAS*, 347, 173
- Sasselov, D. D., & Lecar, M. 2000, *ApJ*, 528, 995
- Tian, F., Toon, O. B., Pavlov, A. A., & De Sterck, H. 2005, *ApJ*, 621, 1049
- Trilling, D. E., Benz, W., Guillot, T., Lunine, J. I., Hubbard, W. B., & Burrows, A. 1998, *ApJ*, 500, 428
- Vassiliadis, E. & Wood, P. 1993, *ApJ*, 413, 641
- Vassiliadis, E. & Wood, P. 1994, *ApJ*, 92, 125
- Vidal-Madjar, A., Lecavelier des Etangs, A., Désert, J.-M., Ballester, G. E., Ferlet, R., Hébrard, G., & Mayor, M. 2003, *Nature*, 422, 143
- Vidal-Madjar, A., et al. 2004, *ApJ*, 604, L69
- Villaver, E., García-Segura, G., & Manchado, A. 2002a, *ApJ*, 571, 880
- Villaver, E., Manchado, A., & García-Segura, G. 2002b, *ApJ*, 581, 1204
- Villaver, E., García-Segura, G., & Manchado, A. 2003, *ApJ*, 585, L49
- Villaver, E., & Stanghellini, L. 2005, *ApJ*, 632, 854
- Waite, J. H., Cravens, T. E., Kozyra, J., Nagy, A. F., Atreya, S. K., & Chen, R. H. 1983, *J. Geophys. Res.*, 88, 6143
- Watson, A. J., Donahue, T. M., & Walker, J. C. G. 1981, *Icarus*, 48, 150
- Yelle, R. V. 2004, *Icarus*, 170, 167
- Zahn, J.-P. 1977, *A&A*, 57, 383
- Zinnecker, H., Correia, S., Brandner, W., Friedrich, S., & McCaughrean, M. 2006, *IAU Colloq. 200: Direct Imaging of Exoplanets: Science Techniques*, 19
- Zuckerman, B., & Becklin, E. E. 1987, *Nature*, 330, 138

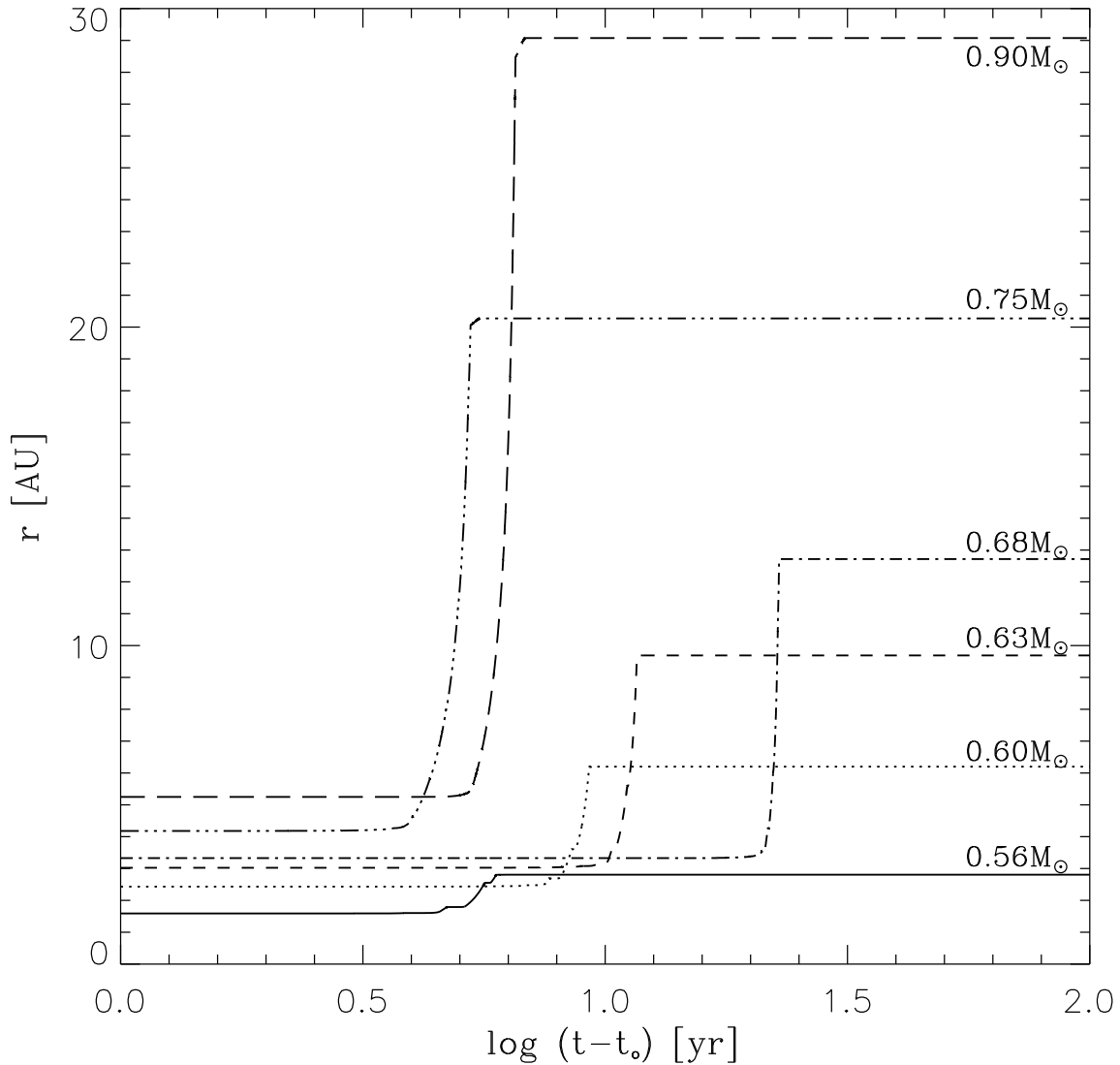


Fig. 1.— Evolution of the orbital distance caused by the stellar mass-loss during the AGB phase. The time is given in logarithmic scale, with t_0 representing the beginning of the AGB evolution. Each curve represent a different PN central star mass, marked on each curve and with different line-styles. We have used an initial orbital distance that equals the maximum radius reached by the star during the AGB phase.

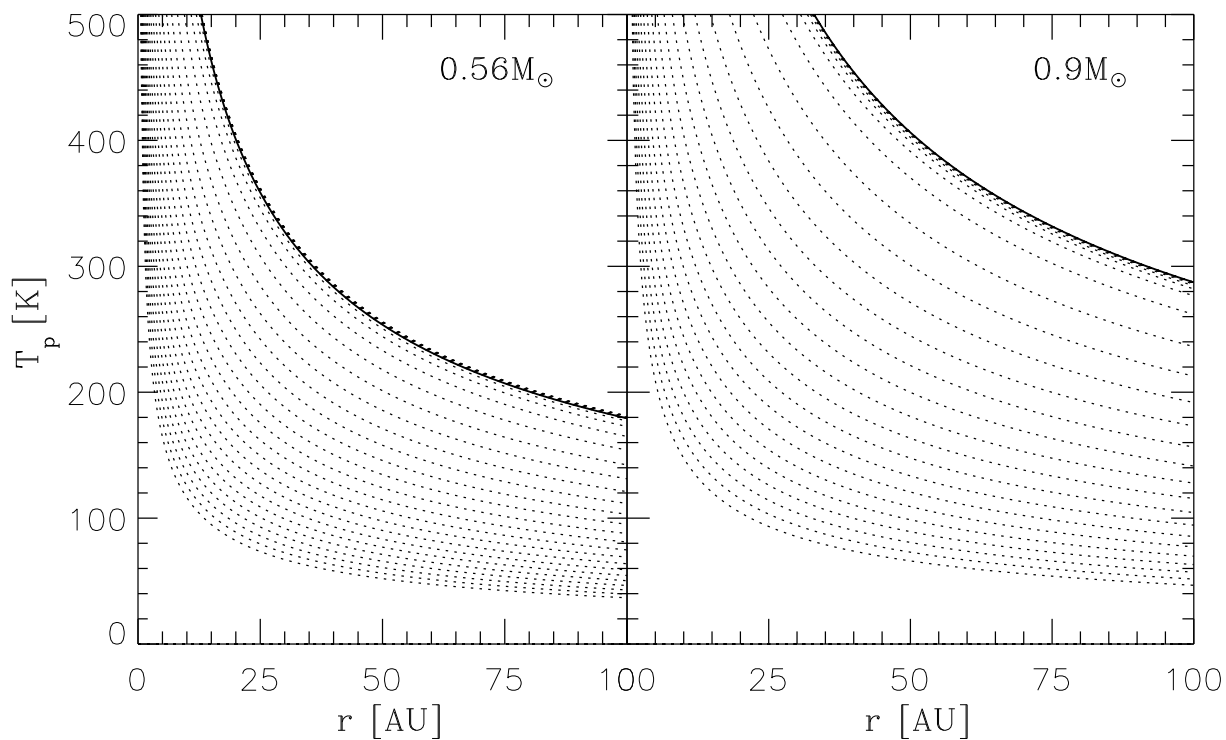


Fig. 2.— Left: the solid line represents the planet’s equilibrium temperature (from Eq. 5) versus orbital distance for a star of $0.56 M_{\odot}$ as it enters the PN phase. The dashed lines follow the evolution of the star up to 1.1×10^6 yr after the PN phase starts. The lowest equilibrium temperature corresponding to the latest point in the evolution. Right: the same for a $0.9 M_{\odot}$ star evolved to 1×10^5 yr into the PN phase.

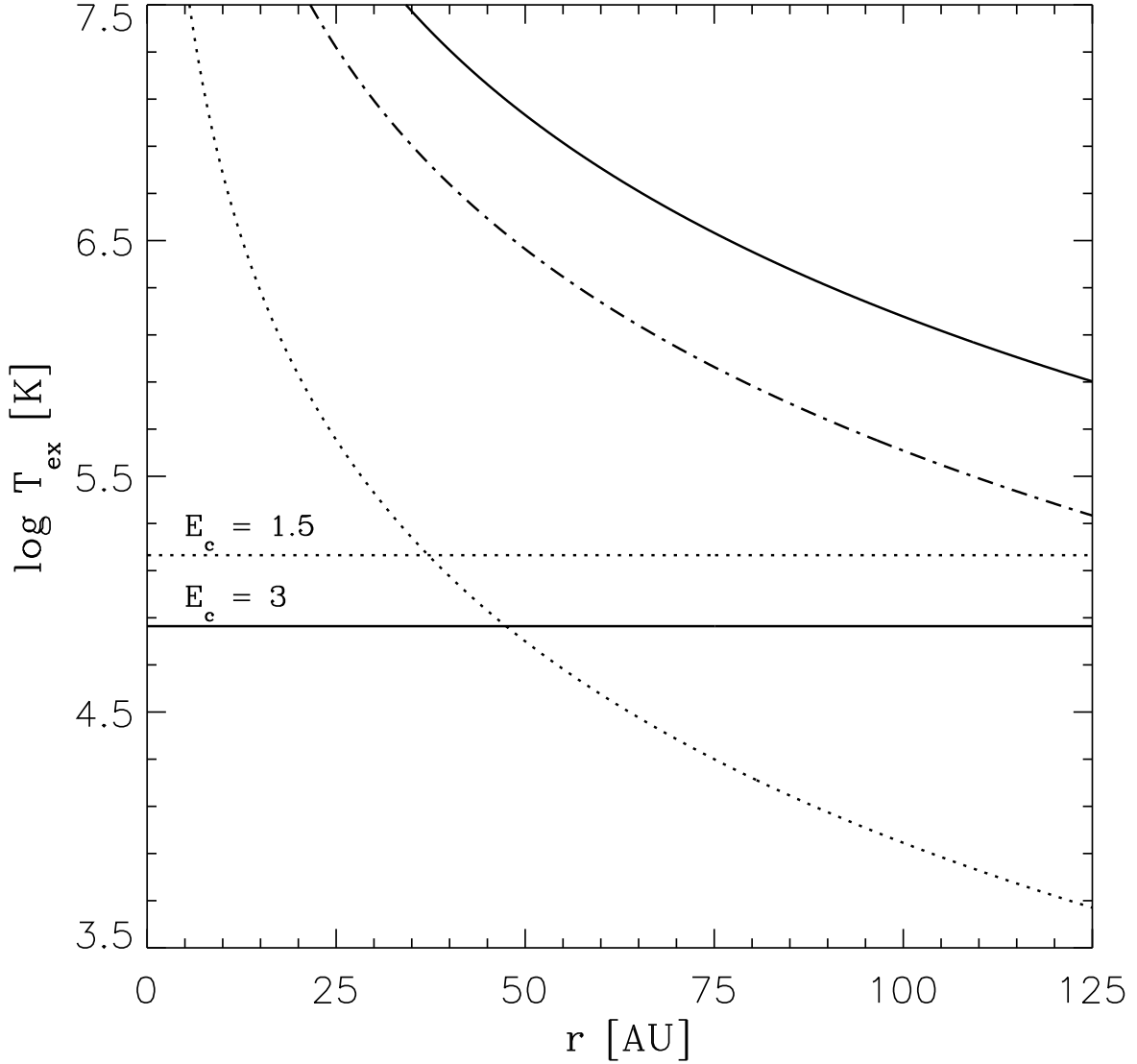


Fig. 3.— Exospheric temperature (in Logarithmic scale) reached at the atmosphere of a $1 M_J$ planet orbiting a $0.56 M_\odot$ star ($1 M_\odot$ main sequence) plotted versus the orbital distance. The different curves (solid, dashed, and dotted) are the result of changing the XUV intensity due to the evolution of the star and are chosen at luminosities of 3.6 , 1.4 and $0.1 \times 10^3 L_\odot$ respectively which correspond to stellar effective temperatures of $36\,000$, $115\,000$ and $96\,000$ K respectively. The solid horizontal line represents T_{ex} , or the escape parameter $E_c=3$ (as defined in the text), above which the atmosphere reaches blow off conditions. The position of $E_c=1.5$ is also shown as a dotted line.

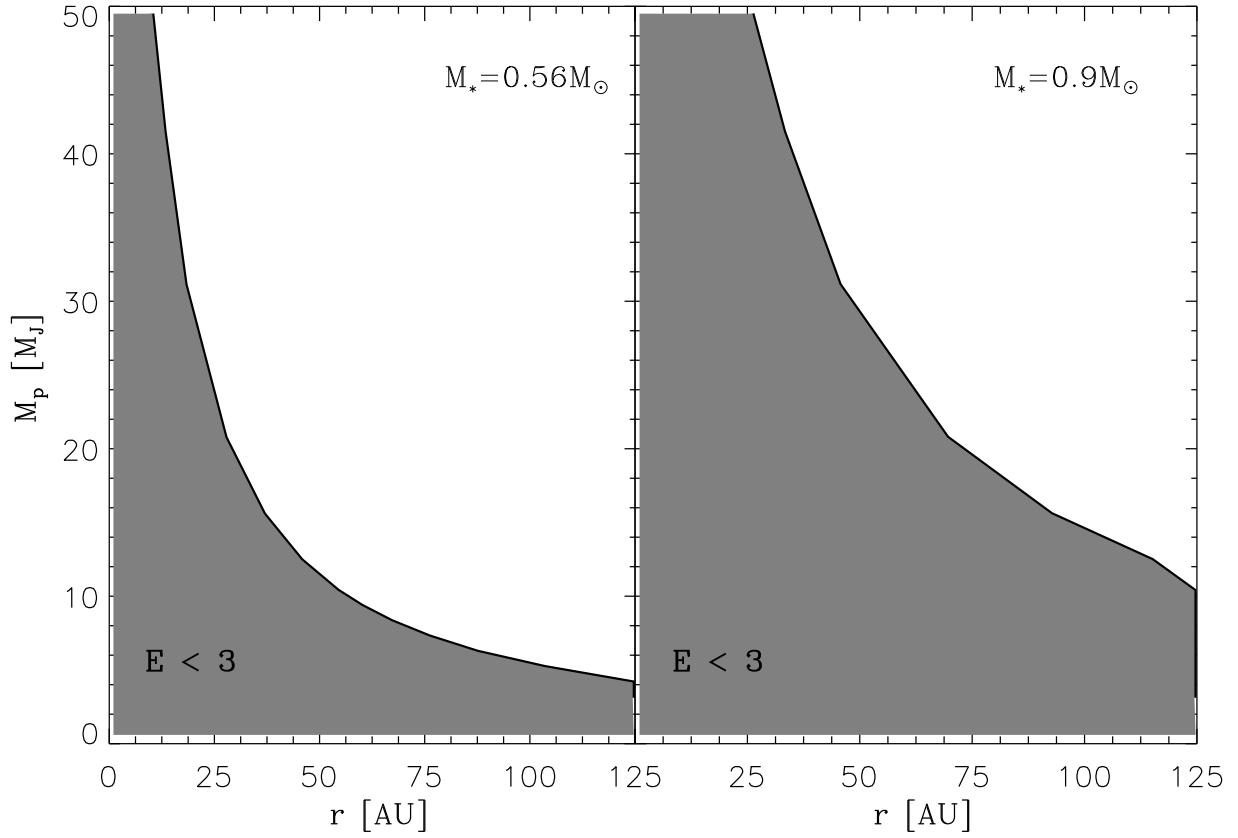


Fig. 4.— The grey area represents the parameter space region (planet’s mass versus orbital distance) for which the planet’s atmosphere reaches blow off conditions using a critical escape parameter, $E_c = 3$. Left: E_c computed for planets embedded in the PN environment created by the lowest mass PN progenitor $0.56 M_\odot$ ($1 M_\odot$ main sequence mass) at an early age, when $L_* = 3.6 \times 10^3 L_\odot$ and $T_{eff} = 36\,000$ K. Right: the same but for a $0.9 M_\odot$ central star.

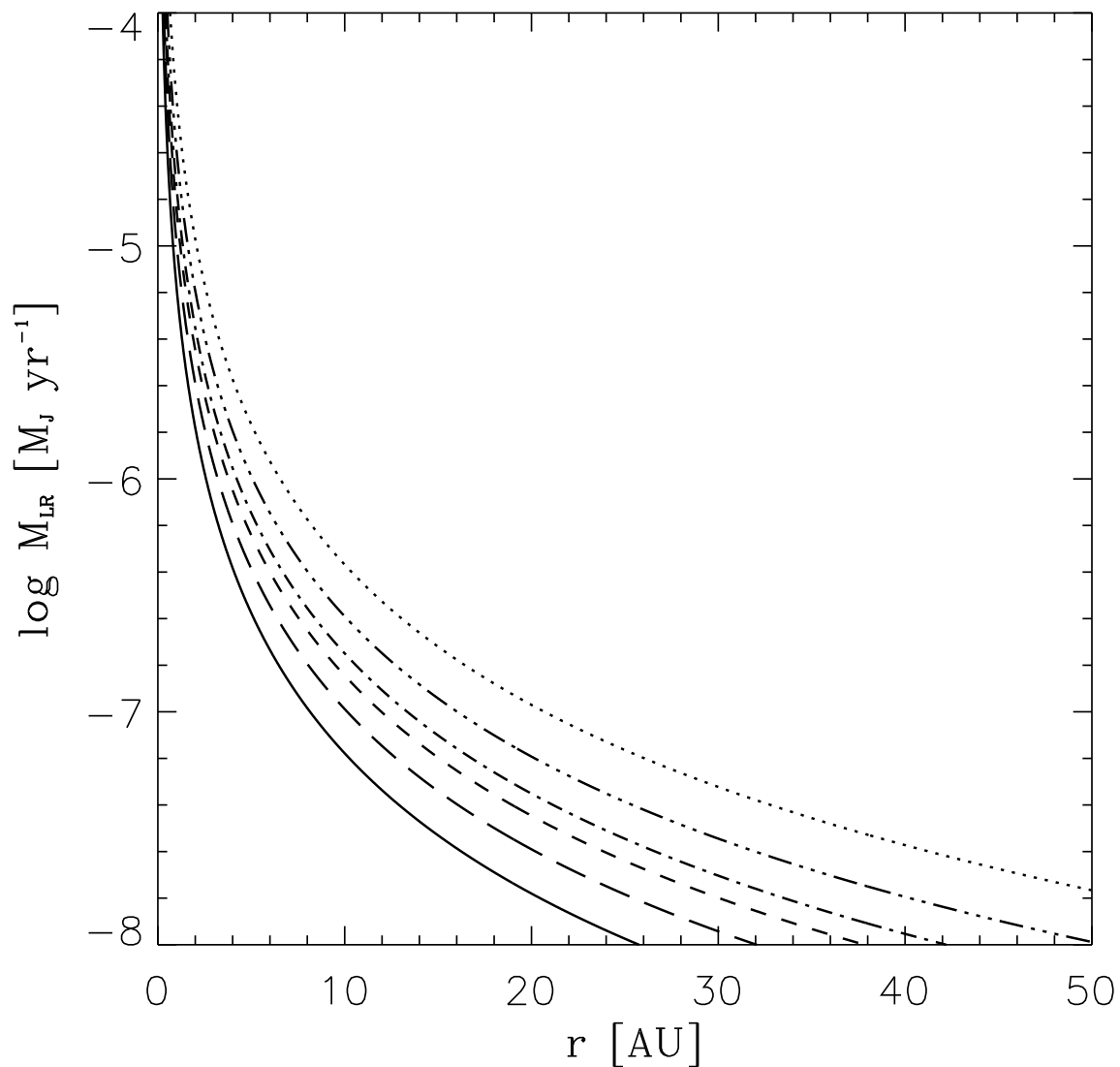


Fig. 5.— Mass-loss using $\xi = 3$ (see text) (in logarithmic scale and $M_J \text{ yr}^{-1}$) versus orbital distance of a Jupiter-like planet under hydrodynamic escape conditions. The solid line is for the radiation field emitted by the lowest mass core 30 000 yr after the star enters the PN phase of evolution. The different lines are for all the other stellar masses considered with the radiation (and therefore the mass-loss rates) increasing with the stellar mass.

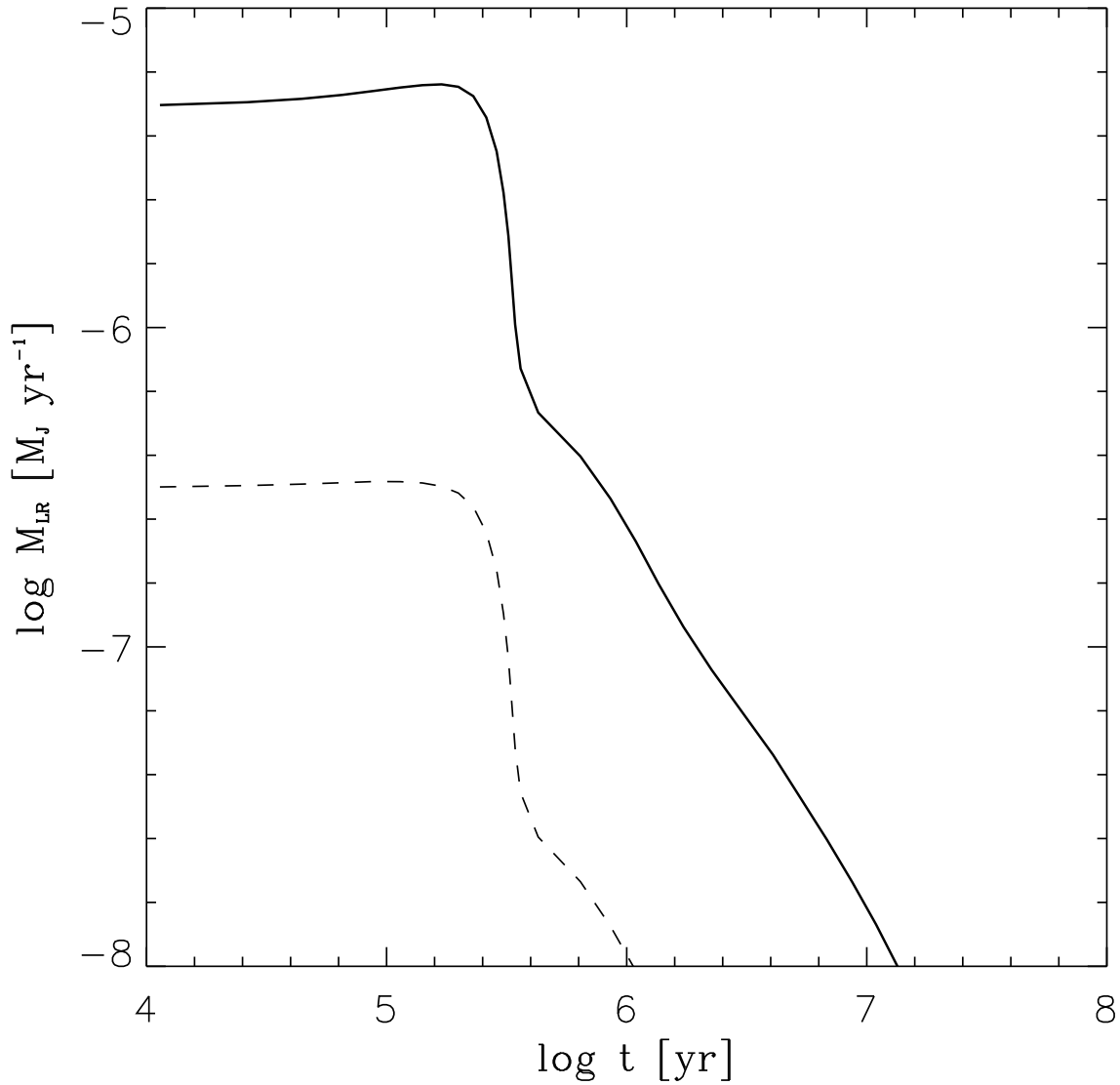


Fig. 6.— The solid line represents the evolution of the evaporation rate (in logarithmic scale and $M_J \text{ yr}^{-1}$) of a $1 M_J$ mass planet under hydrodynamic escape conditions and at a distance of 1.5 AU from a . for a $1 M_{\odot}$ star. The same for the dashed line but for a distance of 5 AU. Time zero is set as the star leaves the AGB phase . The evolution of the stellar luminosity during the PN phase has been taken from the stellar evolutionary models of Vassiliadis & Wood (1994) and it has been extended to the white dwarf cooling sequence using the models of Prada Moroni & Straniero (2002).

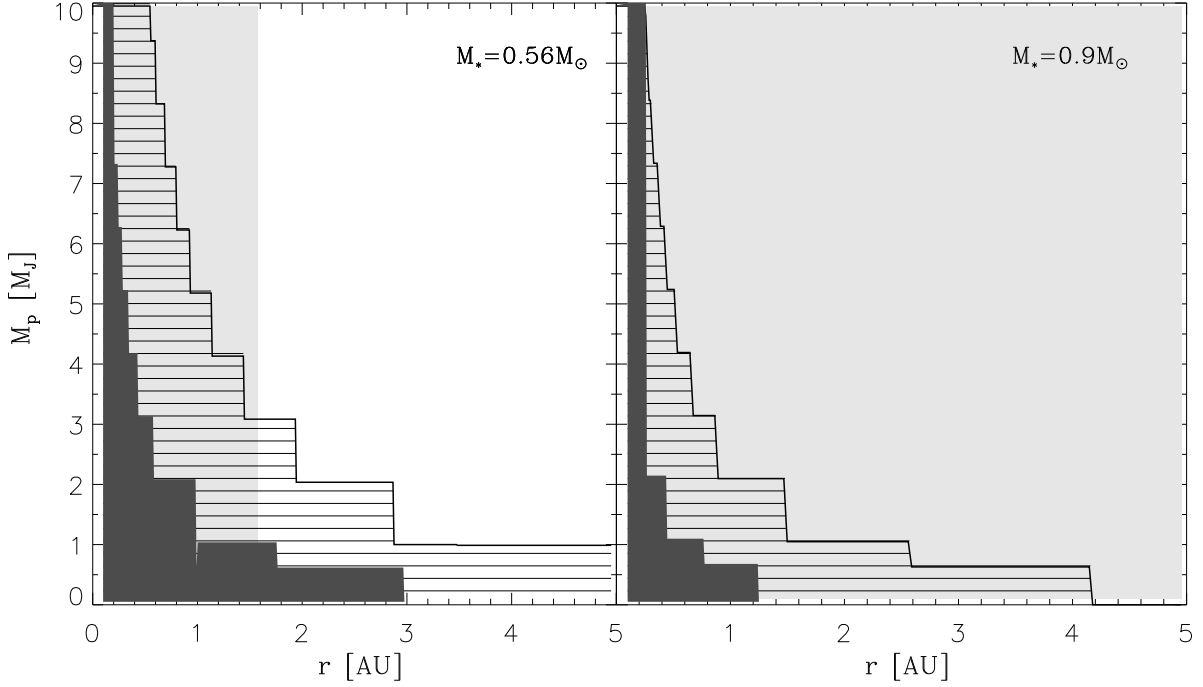


Fig. 7.— Left: The dark gray area represent the region where a planet loses 50 % of its mass when orbiting a $0.56 M_{\odot}$ star by using $\xi = 3$ (see text). The same for the region with parallel line filling but using $\xi = 10$. The light gray area represents the orbital distance reached by the stellar radius during the AGB phase. Right: the same for planets orbiting $0.9 M_{\odot}$ central star.

Table 1. MASSES, ORBITAL DISTANCES

M_{MS} [M_{\odot}]	M_{WD} [M_{\odot}]	R_*^{max} [AU]	$r(t)/r_o$
1.0	0.56	1.59	1.8
1.5	0.60	2.43	2.5
2.0	0.63	3.02	3.2
2.5	0.68	3.33	3.8
3.5	0.75	4.18	4.9
5.0	0.90	5.25	5.5

Table 2. % EVAPORATION FOR 0.56 M_{\odot} STAR

$M_p[M_J]$	r[AU]	$\xi=3$	$\xi=5$	$\xi=10$
1	1	100 %	100 %	100 %
	2	30 %	100 %	100 %
	3	20 %	40 %	100 %
	4	10 %	20 %	100 %
	5	5 %	20 %	70 %
	10	1 %	5 %	20 %
5	1	4 %	10 %	52 %
	2	1 %	3 %	10 %
	3	0.4 %	1 %	5 %
	4	0.2 %	0.6 %	3 %
	5	0.1 %	0.4 %	1.6 %
	10	0.04 %	0.1 %	0.4 %